Virologica Sinica (2019) 34:508–520
https://doi.org/10.1007/s12250-019-00141-0

www.virosin.org
www.springer.com/12250

RESEARCH ARTICLE

SNX11 Identified as an Essential Host Factor for SFTS Virus Infection by CRISPR Knockout Screening

Tiezhu Liu[1] · Jiajia Li[3,4] · Yang Liu[1] · Yuanyuan Qu[1] · Aqian Li[1] · Chuan Li[1] · Quanfu Zhang[1] · Wei Wu[1] · Jiandong Li[1] · Yan Liu[3] · Dexin Li[1] · Shiwen Wang[1,2] · Mifang Liang[1,2]

Received: 22 March 2019 / Accepted: 17 May 2019 / Published online: 18 June 2019

Abstract

Severe fever with thrombocytopenia syndrome virus (SFTSV) is a highly pathogenic tick-borne bunyavirus that causes lethal infectious disease and severe fever with thrombocytopenia syndrome (SFTS) in humans. The molecular mechanisms and host cellular factors required for SFTSV infection remain uncharacterized. Using a genome-wide CRISPR-based screening strategy, we identified a host cellular protein, sorting nexin 11 (SNX11) which is involved in the intracellular endosomal trafficking pathway, as an essential cell factor for SFTSV infection. An SNX11-KO HeLa cell line was established, and SFTSV replication was significantly reduced. The glycoproteins of SFTSV were detected and remained in later endosomal compartments but were not detectable in the endoplasmic reticulum (ER) or Golgi apparatus. pH values in the endosomal compartments of the SNX11-KO cells increased compared with the pH of normal HeLa cells, and lysosomal-associated membrane protein 1 (LAMP1) expression was significantly elevated in the SNX11-KO cells. Overall, these results indicated that penetration of SFTSV from the endolysosomes into the cytoplasm of host cells was blocked in the cells lacking SNX11. Our study for the first time provides insight into the important role of the SNX11 as an essential host factor in the intracellular trafficking and penetrating process of SFTSV infection via potential regulation of viral protein sorting, membrane fusion, and other endocytic machinery.

Keywords CRISPR screen · Severe fever with thrombocytopenia syndrome virus (SFTSV) · Host factor · Sorting nexin 11 (SNX11)

Introduction

Severe fever with thrombocytopenia syndrome virus (SFTSV), a novel highly pathogenic bunyavirus, was first discovered in the Dabie Mountains in China (Yu *et al.* 2011) and causes severe fever with thrombocytopenia syndrome (SFTS), which is a life-threatening emerging infectious disease with an initial case fatality rate of 30%. SFTSV infections have been reported in over 26 provinces in China (Zhan *et al.* 2017), Japan (Takahashi *et al.* 2014), and South Korea (Kim *et al.* 2013). Similar viruses have also been reported in the US (McMullan *et al.* 2012). Since the initial discovery of SFTSV, the expanding endemic infection of SFTSV has become more important and significant as a global public health concern. Currently, there are no vaccines or specific antivirals available against SFTSV infection. Because of limited information, SFTSV entry, penetration, replication, and maturation require

Electronic supplementary material The online version of this article (https://doi.org/10.1007/s12250-019-00141-0) contains supplementary material, which is available to authorized users.

✉ Shiwen Wang
wangsw@ivdc.chinacdc.cn

✉ Mifang Liang
liangmf@ivdc.chinacdc.cn

[1] Key Laboratory of Medical Virology and Viral Diseases, Ministry of Health of People's Republic of China, National Institute for Viral Disease Control and Prevention, Chinese Center for Disease Control and Prevention, Beijing 102206, China

[2] CDC-WIV Joint Research Center for Emerging Diseases and Biosafety, Wuhan 430071, China

[3] Department of Microbiology, Anhui Medical University, Hefei 230032, China

[4] The First Affiliated Hospital of Anhui Medical University, Hefei 230022, China

further investigation to understand the molecular mechanisms involved.

Usually, members of the *Bunyavirales* Order gain access to the host cells by endocytosis via clathrin-dependent or independent pathways (de Boer *et al.* 2012; Mayor *et al.* 2014). When the virus enters the host cells, the virions are internalized from the plasma membrane and can follow the endocytic membrane trafficking pathway to Rab5+ early endosome, RAB7a+ late endosomes, and the lysosomal-associated membrane protein 1 (LAMP1+) endolysosomes (Jin *et al.* 2002; Lozach *et al.* 2010). Following endocytosis, viral penetration could be proceeded through the acidification of the endocytic vesicles and conformational changes in glycoproteins Gn and/or Gc of bunyavirus, finally triggering membrane fusion between the viral and endosomal membrane. This could be followed by release of viral genome and polymerase to the cytoplasm for the next steps of viral replication, assembly, and maturation (Plegge *et al.* 2016; Tani *et al.* 2016). The entry of SFTSV has been shown to use the clathrin-dependent endocytic pathway by recruiting clathrin into the cell membrane for the formation of clathrin-coated pits during receptor-mediated endocytosis (Liu *et al.* 2018). A previous study showed that SFTSV used DC-SIGN or DC-SIGN-related (DC-SIGNR) as receptors (Tani *et al.* 2016); however, many SFTSV susceptible cell lines did not express lectins. Non-muscle myosin heavy chain IIA entry (NMMHC-IIA) was reported to be an SFTSV receptor which contributes to viral entry (Sun *et al.* 2014). Another report showed that entry of SFTSV was mediated by SFTSV glycoproteins and depended on dynamin, which is essential for the formation of clathrin-coated pits from the plasma membrane and that SFTSV entry was pH-dependent (Hofmann *et al.* 2013; Tani *et al.* 2016). Limited information is currently available regarding the intracellular trafficking processes of SFTSV infection and other related cellular factors. A recent study utilizing quantum dot (QD)-based single-particle tracking and imagining methods showed that SFTSV virions were trafficked to early endosomes and then sequentially to late endosomes. Further, membrane fusion occurred in late endosomes triggered by the acidic environment (Liu *et al.* 2018). However, the precise location of SFTSV penetration and the host cellular factors involved in SFTSV trafficking and membrane fusion have remained largely uncharacterized.

The CRISPR–Cas9 based screening system has recently been developed as a tool for gene editing in mammalian cells (Ma *et al.* 2015; Zhang *et al.* 2016; Han *et al.* 2018). Since this system allows for easy knockout of both alleles in a substantial percentage of the treated cells using a high-complexity, genome-wide sgRNA library, it has wide-ranging potential to screen host cell factors which may play important roles in various intracellular trafficking pathways during the process of viral infection. With this novel screening method, a number of cellular genes associated with endocytosis, transmembrane processing, and endoplasmic reticulum (ER) pathways have been identified for infections of flaviviruses including West Nile, Dengue, Zika, yellow fever, Japanese encephalitis, and hepatitis C viruses. Screens for other viruses, such as Human immunodeficiency virus (HIV) (Park *et al.* 2017) and influenza viruses (Heaton *et al.* 2017), have identified host factors involved in virus entry such as sialic acid biosynthesis and related glycosylation pathways. However, very few screens for bunyavirus infection have been performed, and the various host proteins involved in the intracellular pathways of this infection remain unexplicated. In this study, genome-wide CRISPR-based screening methods were utilized to identify host factors for SFTSV infection.

Materials and Methods

Cells and Viruses

Cell lines (HeLa, HEK293FT, and Vero cells) were initially acquired from the American Type Culture Collection (ATCC; USA). They were cultured at 37 °C under 5% CO_2 in Dulbecco's modified Eagle's medium (DMEM; Life Technologies, USA) supplemented with 10% heat-inactivated fetal bovine serum (FBS; Life Technologies, USA) and 1% penicillin/streptomycin (Life Technologies, USA). Cells were passaged every 2 days and digested with 0.05% trypsin–EDTA. SFTSV strain HB29 was first isolated in our laboratory (Yu *et al.* 2011), then passaged in Vero cells as a virus stock, and further utilized to infect Hela cells at an MOI of 0.5 for the CRISPR screen and the validation experiments and an MOI of 100 for the confocal microscopy analysis.

Lentivirus Production and Titer

The GeCKO v2 human library in lentiCRISPR v2 containing 64,751 single guide RNAs (sgRNAs) targeting 18,080 protein-coding human genes was derived by the Zhang laboratory (Zhang *et al.* 2016), obtained from a commercial source (Addgene, USA), and was amplified in Endura Electro Competent cells (Lucigen, USA). Briefly, HEK293FT cells were seeded into 6-well plates, grown to 80% confluence, and then transfected with the pooled sgRNA library, and then, lentiviral helper plasmids (pMD2.G and psPAX2) were utilized for lentivirus production. Lentiviruses were harvested at 36 and 60 h post transfection and concentrated by centrifugation at 1500 $\times g$ for 15 min. The supernatant was filtered with a 0.45 μm Stericup® Filter Unit (Millipore, USA). Lentiviral

titer was determined with the Lenti-Pac™ HIV qRT-PCR Titration Kit (GeneCopoeia, USA).

Lentiviral Transfection and Screening

HeLa cells were seeded into 12-well plates at a density of 3×10^6 cells in 2 mL of DMEM per well with 8 μg/mL Polybrene® (Sigma-Aldrich, USA) and then spinfected with the sgRNA lentivirus library at a MOI of 0.2 for 2 h at 25 °C, followed by incubation at 37 °C for 8 h. The supernatant was replaced with 2 mL of DMEM containing 2% FBS, 1% penicillin/streptomycin, and 1 μg/mL puromycin, which was used to select the transduced cells. Following puromycin treatment for 5 days, the survived cells were dissociated with 0.05% trypsin–EDTA, pooled in T75 cell culture flasks, and incubated at 37 °C for 2 days. They were then dissociated with 0.05% trypsin–EDTA, diluted 1:500,000 cell in each well, and seeded in 96-well plates with 100 μL of cell suspension per well. After the cells formed clones, they were dissociated with 0.05% trypsin–EDTA and suspended with 200 μL of fresh cell culture medium. The cell suspension from 96-well plates was divided and duplicated into two 96-well plates and grown to 80% confluence. The cells were infected with SFTSV at a MOI of 0.5 and subjected to ELISA 4 days after infection; then, the SFTSV nucleoprotein (NP) in the supernatant was detected to screen whether the cells were resistant to this viral infection. The cells in the negative wells were collected, and the corresponding genomic DNA was extracted with the Blood and Cell Culture DNA Midi Kit (Qiagen, Germany) and used for next-generation sequence analysis.

PCR Amplification for the Integrated sgRNA, Sequencing, and Analysis

PCR amplification of the genomic DNA (2 μg) collected above was performed to amplify the target fragment integrated with sgRNA with the specifically designed primers (Forward: 5′-TTCATATTTGCATATACGATAC; Reverse: 5′-GGGACTGTGGGCGATGT). The PCR products were then purified with the QIAquick PCR Purification Kit (Qiagen, Germany) and quantified with a Qubit 3.2.1 fluorometer (Life Technologies, USA). The purified products (100 ng) were end-repaired. Then, adaptor ligation and size selection with E-Gel SizeSelect Agarose Gel (Invitrogen, USA) was performed. The amplicon library (650 pM) was added to the emulsion PCR amplification solution and sequenced using the Ion Personal Genome Machine (PGM) System (Life Technologies, USA). Finally, the MAGeCK algorithm was used to analyze the raw data following sequencing.

Generation of the SNX11-KO Cell Line

The sgRNA (5′-CACCGCCGCTACCGTGAGTTCGTG-3′) targeted to SNX11 was inserted into the backbone plasmid of lentiCRISPR-v2 vector (Addgene plasmid 52,961) at the *Bsp3I* site. Constructs were co-transfected using Lipofectamine 3000 into HEK293FT cells with lentiviral helper plasmids (pMD2.G and psPAX2). The lentiviruses produced above were used to transfect HeLa cells, followed by puromycin selection at 1 μg/mL for 5 days post-transfection. Following removal of puromycin, the cells were allowed to recover for 2 days and were diluted into 96-well plates containing one cell per well. Cells were cultured at 37 °C under 5% CO_2 for 8 days, transferred to 24-well plates for 2 days, and subjected to sequencing for the target sequence. Finally, the SNX11-gene edited cell line (SNX11-KO) was generated and then later utilized for functional analysis.

To assess re-expression of SNX11 in SNX11-KO HeLa cells, we cloned the *SNX11* gene into the expression vector pcDNA3.1 and transfected and expressed the *SNX11* gene into the SNX11-KO cell line (SNX11-KO^{Plus} cells).

Cell Viability Assay

Wild-type and SNX11-KO Hela cells were seeded into 96-well plates containing 100 μL/well of cell culture medium and incubated in a 37 °C incubator overnight. Then, 10 μL of the cell viability reagent (Invitrogen, USA) was directly added to each well, followed by incubation for 10 min at 37 °C, protected from direct light with tin-foil. Finally, we recorded the absorbance values at 570 nm and used the values to compare cell viability between the wild-type and SNX11-KO cells.

Enzyme-Linked Immunosorbent Assay (ELISA)

ELISA was performed 96 h after infection for the CRISPR-based screen in the 96-well plates. 96-well plates were coated with a rabbit polyclonal antibody directed against the whole SFTSV (500 ng per well); the plates were incubated at 4 °C overnight, then washed with PBS-Tween 20 (PBST), and blocked with 5% skim milk in PBS for 1 h at 37 °C. Culture supernatants, together with the Triton X-100 (diluted 1:1000), were added to the coated 96-well plates and incubated at 37 °C for 1 h. After five washes, a horseradish peroxidase (HRP)-labeled mouse monoclonal antibody against SFTSV nucleoprotein was added, and the plates were incubated at 37 °C for 1 h. Plates were washed five times, and the substrate 3,3′,5,5′-tetramethylbenzidine (TMB) in citrate buffer was added to each well. The addition of 2 N H_2SO_4 stopped the reactions, then optical

densities (at 450 nm) were determined with an ELISA reader (Thermo Scientific, USA). The lower limit of positivity (cut-off) was deemed to be the mean OD plus two standard deviations of the three negative control samples.

The wild-type, SNX11-KO, and SNX11-KO cells were transfected with SNX11 (SNX11-KO^{Plus}) in 24-well plates were infected with SFTSV (MOI 0.5) and cultured for 4, 5, or 6 days. The culture supernatant was harvested and assayed for SFTSV nucleoprotein expression. Each sample was assayed as four replicates. The remaining details were the same as the CRIPSR screen by ELISA described above.

RNA Sequencing

The total RNA found in SNX11-KO HeLa and wild-type cells was isolated with the RNeasy Plus Mini Kit (Qiagen, Germany). Samples were submitted to BGI for sample preparation and sequencing.

Western Blotting Analysis

Expression of SNX11 protein in the wild-type, SNX11-KO, and SNX11-KO^{Plus} cells, was subjected to Western blotting analysis. SNX11-KO^{Plus} cells were collected at 36 h after transfection of SNX11 while SNX11-KO and wild-type cells were also collected. Cells were rinsed once with ice-cold PBS, trypsinized, resuspended in PBS, and the cell suspensions were spun down and resuspended in RIPA buffer, vortexed vigorously for 1 min, and centrifuged at 10,000 $\times g$ for 5 min. Following denaturation at 100 °C for 10 min, an equal amount of each sample was fractionated by 10% SDS-PAGE gel. Separated proteins were transferred to a polyvinylidene difluoride (PVDF) membrane (Bio-Rad, USA) which had been blocked with 5% skim milk in PBS for 1 h. The membrane was incubated overnight at 4 °C with a rabbit polyclonal antibody directed against SNX11 (Novus, USA), and then washed three times with 1 × PBST. β-actin detected with a rabbit anti-β-actin antibody (Cell Signaling Technology, USA) was utilized as the loading control. The membrane was then incubated with an HRP-conjugated secondary antibody for 1 h and washed three times with PBST for 10 min each.

A rabbit polyclonal antibody directed against LAMP1 (Abcam, UK) was used to assess increases in LAMP1 expression, and then used as the primary antibody and then the remaining details were the same as those analysis of SNX11 expression described above.

Confocal Microscopy and Immunofluorescence

For preparation for confocal microscopy, HeLa cells were loaded into 8-well glass slides and infected with SFTSV at an MOI of 100 after they had grown to 80% confluence. Then, cells were fixed with 4% paraformaldehyde at 48 h post-infection. This time period was selected because our previous experiments had found that the SFTSV GP positive cells were generally not found until 48 h after infection due to the limited susceptibility of the HeLa cells. Then, cells were permeabilized with 0.25% Triton X-100 for 30 min at room temperature and blocked with PBS containing 3% bovine serum albumin for 1 h at room temperature. Cells were then stained overnight at 4 °C with a mouse monoclonal antibody targeted at SFTSV GP, together with the following a rabbit anti-RAB5a (early endosome; Cell Signaling Technology, USA), anti-RAB7a (late endosome; Cell Signaling Technology, USA), anti-LAMP1 (late endosomal compartments, Abcam, UK), anti-PDI (ER; Cell Signaling Technology, USA), and anti-RCAS1 (Golgi apparatus; Cell Signaling Technology, USA), respectively. Cells were then stained with a secondary anti-rabbit IgG antibody conjugated with Alexa Fluor 488 or Alexa Fluor 594, together with an anti-mouse IgG antibody conjugated with Alexa Fluor 594 or Alexa Fluor 488, for 30 min at room temperature. Cells were then washed three times and stained with 4,6-diamidino-2-pheny-indole (DAPI; Cell Signaling Technology, USA) for 10 min at room temperature. Finally, cells were observed with a Leica TCS SP8 laser scanning confocal microscope (Leica, Germany), and the resultant images were acquired with a 63× objective.

A rabbit polyclonal antibody against SNX11 was used for immunofluorescence analysis of SNX11 expression. Rabbit polyclonal antibody was the primary antibody and an anti-rabbit IgG antibody conjugated with Alexa Fluor 488 was utilized as the secondary antibody.

Flow-Cytometric Analysis

HeLa cells infected with SFTSV at a MOI of 0.5 were fixed with IC Fixation Buffer (Invitrogen, USA) for 15 min, washed three times with PBS, and permeabilized with eBioscience^{TM} Permeabilization Buffer (Invitrogen, USA) for 30 min before they were stained with rabbit polyclonal antibody against the whole SFTSV as the primary antibody and goat anti-rabbit antibody as a secondary antibody. Finally, the cells were suspended within 1 mL ice-cold PBS and subjected to detection.

For the detection of RAB5a, RAB7a, and LAMP1 expression, the details were the same as analysis of SFTSV positive rate described above. The data were visualized and processed with the Flow Jo software.

Electron Microscopy

Monolayers of SNX11-KO and wild-type HeLa cells were fixed for transmission electron microscopy. Ultrathin sections were cut with a Reichert-Leica Ultracut S Ultramicrotome (Austria), stained with lead citrate, and examined with a Philips 201 electron microscope (Holland) at 60 kV.

Results

CRISPR–Cas9 Based Screening to Identify Genes Essential for SFTSV Infection

We designed a screening strategy, illustrated in Supplementary Figure S1 to investigate host cellular genes essential for SFTSV infection. GeCKO lentivirus library was generated by transfecting HEK293FT cells with lentiCRISPR-v2 library together with lentiviral helper plasmids (pMD2.G and psPAX2). CRISPR–Cas9 gene knockout screening was performed in 96-well plates. HeLa cells were infected with the lentivirus library at a low MOI to ensure that the majority of cells received only one genetic perturbation and were diluted and calculated to nearly a single cell per well, and then seeded into 96-well plates after a puromycin selection, followed by SFTSV infection. Supernatants of each well were detected for viral infection. Finally, we selected cells from 8 wells with low viral nucleoprotein found in the supernatants, and their OD450 values ranged from 0.148 to 0.239, compared to the positive control (OD450 value = 2.155) (Table 1). Then, the integrated sgRNA fragments of the selected cells were PCR amplified. Amplified products were subjected to deep sequencing, and candidate genes were identified and ranked using model-based analysis of the genome-wide CRISPR/Cas9 knockout (MAGeCK) program. Results found that the majority of the cells from selected wells in which the cells were resistant to SFTSV infection presented multiple sgRNAs inserts, and only one well (Sample 1) showed a dominant gene for SNX11 with a percentage of 99.79% (Table 1). Because the relationship between SFTSV infection and the genes detected in these wells had not yet been clarified, we selected only SNX11, which was closely related to the endocytic pathway for further functional analysis in this study. In order to verify the SFTSV resistance of cells with the SNX11 knockout, we cloned SNX11 sgRNA into the backbone plasmid vector of lentiCRISPR v2 and then transfected the HeLa cells. A single SNX11 knockout cell line (SNX11-KO) was established by utilizing the CRISPR/cas9 system, and then the sequence was analyzed. As depicted in Fig. 1A, the sgRNA target site of the *SNX11* gene was fully clipped and disrupted the complete gene. Knockout efficiency was confirmed with Western blotting (Fig. 1B) and immunofluorescence (Fig. 1C), and both showed a lack of SNX11 protein expression in SNX11-KO cells. We performed a cell viability assay in order to investigate whether the knockout of SNX11 affected cell viability and no significant differences in cell viability were found between WT and SNX11-KO cells (Supplementary Figure S2).

Further, we cloned the *SNX11* gene into the expression vector pcDNA3.1, and transfected and expressed the *SNX11* gene into the SNX11-KO cell line; then protein expression was confirmed with Western blotting (Fig. 2A). Cells of the wild-type, SNX11-KO, and SNX11-KO^{Plus} were infected with SFTSV followed by detection of viral RNA in infected supernatants with real-time PCR at 96, 120, and 144 h post infection. These results showed that SFTSV RNA load significantly decreased in the SNX11-KO cell supernatants and was recovered in the SNX11-KO^{Plus} cells (Fig. 2B). SFTSV NP protein expression also significantly decreased in the SNX11-KO cells and was recovered in the SNX11-KO^{Plus} cells via ELISA detection (Fig. 2C). Flow cytometry was also used to compare the infection rates, and the results showed that in wild-type cells, the SFTSV infection rate was 0.01%, 3.37%, 24.43%, 36.21% at 0, 96, 120, 144 h post-infection respectively (Fig. 2D, left panel), which decreased to 0.03%, 0.28%, 0.88%, 5.55% in the SNX11-KO cells (Fig. 2D, middle panel). During re-expression of SNX11, the infection rates recovered to 0.01%, 2.51%, 13.02%, 32.28% in the SNX11-KO^{plus} cells (Fig. 2D, right panel). Fluctuating infection rates caused by the knockout and re-expression of SNX11 indicated that SNX11 was required in order to establish this viral infection within the host.

SNX11-Knockout Blocked the Penetration of SFTSV into the Cytoplasm

To investigate the precise position where SFTSV infection was blocked, we performed a confocal-microscopic analysis to investigate the colocalization between SFTSV and various organelle markers in the SNX11-KO and the wild-type cells. First, we infected two kinds of cells with SFTSV and fixed the cells at 48 h post infection. Cells were permeabilized and blocked. Next, we chose a glycoprotein (GP) of SFTSV required throughout the life cycle of this virus. Then, the sample was stained with mouse monoclonal antibody directed against SFTSV GP and rabbit antibodies against a series of organelle markers and stained with a secondary antibody. Our results found that the infection rate of the SNX11-KO cells was lower than that of the wild-type cells, which was consistent with the validation results above, and therefore, only the cells that were SFTSV GP positive were utilized for confocal microscopic

Table 1 Results of deep sequencing of sgRNAs in SFTSV negative cells.

Sample	Anti-NP ELISA (OD450 value)	Total sgRNA reads	Genes	sgRNA reads	Percentage
1	0.204	2,705,450	SNX11	2,700,017	99.79
2	0.148	862,251	KRIT1	691,567	80.20
			LRRC31	129,920	15.07
3	0.186	201,987	SRRD	105,551	52.26
			DAND5	56,433	27.94
4	0.152	767,552	ZBTB6	448,375	58.42
			BOC	144,551	18.83
5	0.239	1,222,401	PTPN11	497,070	40.66
			PRSS37	496,690	40.63
6	0.201	561,712	KRTAP5-3	234,977	41.83
			Hsa-mir-5589	215,497	38.36
7	0.148	635,352	AHR	421,470	66.34
			PLA2R1	126,433	19.90
8	0.196	1,129,315	CLDN19	391,174	34.64
			DHPS	371,174	32.87
			MIXL1	243,098	21.53

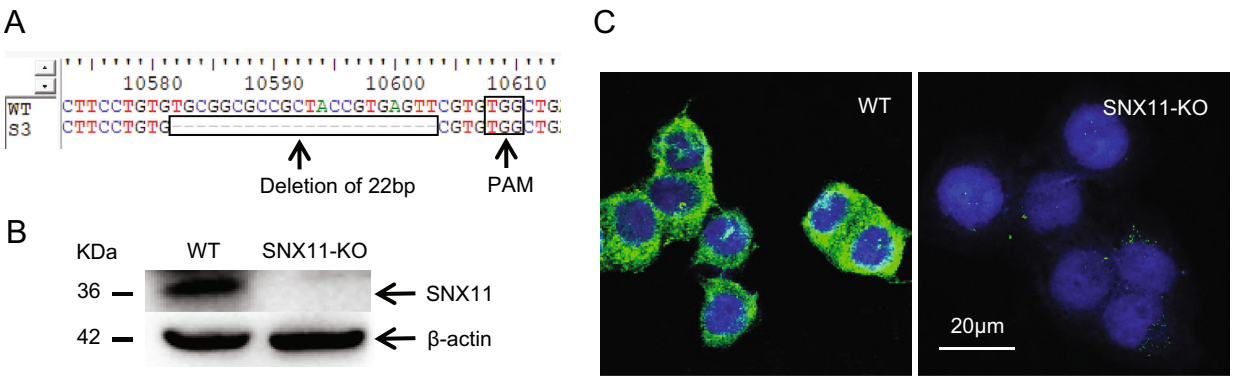

Fig. 1 SNX11 knockout efficiency. **A** Sequence analysis of the SNX11-KO cell line. SNX11-KO represents one SNX11 knockout cell line. The target and a protospacer adjacent motif (PAM) sequence are highlighted in black boxes. **B** Western blotting confirmed the efficiency of the SNX11 knockout. β-Actin was used as the loading control. **C** Immunofluorescence assay (IFA) indicated that there was no expression of SNX11 in SNX11-KO cells.

analysis. Our results showed that in wild-type cells, SFTSV GP colocalized with RAB5a+ early endosome (Fig. 3A, upper panel), RAB7a+ late endosome (Fig. 3B, upper panel), LAMP1+ endolysosome, or the lysosome (Fig. 3C, upper panel), suggesting that normally SFTSV would enter the early endosome, late endosome, endolysosome, or lysosome. Furthermore, in wild-type cells, SFTSV GP could colocalize with protein disulfide isomerase (PDI), an ER marker (Fig. 3D, upper panel), and receptor binding cancer antigen expressed in SiSo cells (RCAS1), a Golgi apparatus marker (Fig. 3E, upper panel), which suggested that SFTSV could penetrate the endolysosome into the cytoplasm. During RNA replication, synthesis and dimerization of Gn and Gc in the ER and glycosylation of the viral protein in the Golgi apparatus proceeded. However, in SNX11-KO cells, SFTSV GP could only colocalize with RAB5a (Fig. 3A, lower panel), RAB7a (Fig. 3B, lower panel), and LAMP1 (Fig. 3C, lower panel), but could not colocalize with PDI (Fig. 3D, lower panel) and RCAS1 (Fig. 3E, lower panel), which indicated that the knockout of SNX11 did not affect trafficking of SFTSV from the early endosome to the endolysosome but affected the penetration of SFTSV into the cytoplasm and affected the process of SFTSV GP synthesis as well as maturation in the ER. Since SNX11 was primarily an intracellular trafficking protein which mostly localized in the endosomal membrane, we speculated that the knockout of SNX11 could block the penetration of SFTSV into the cytoplasm.

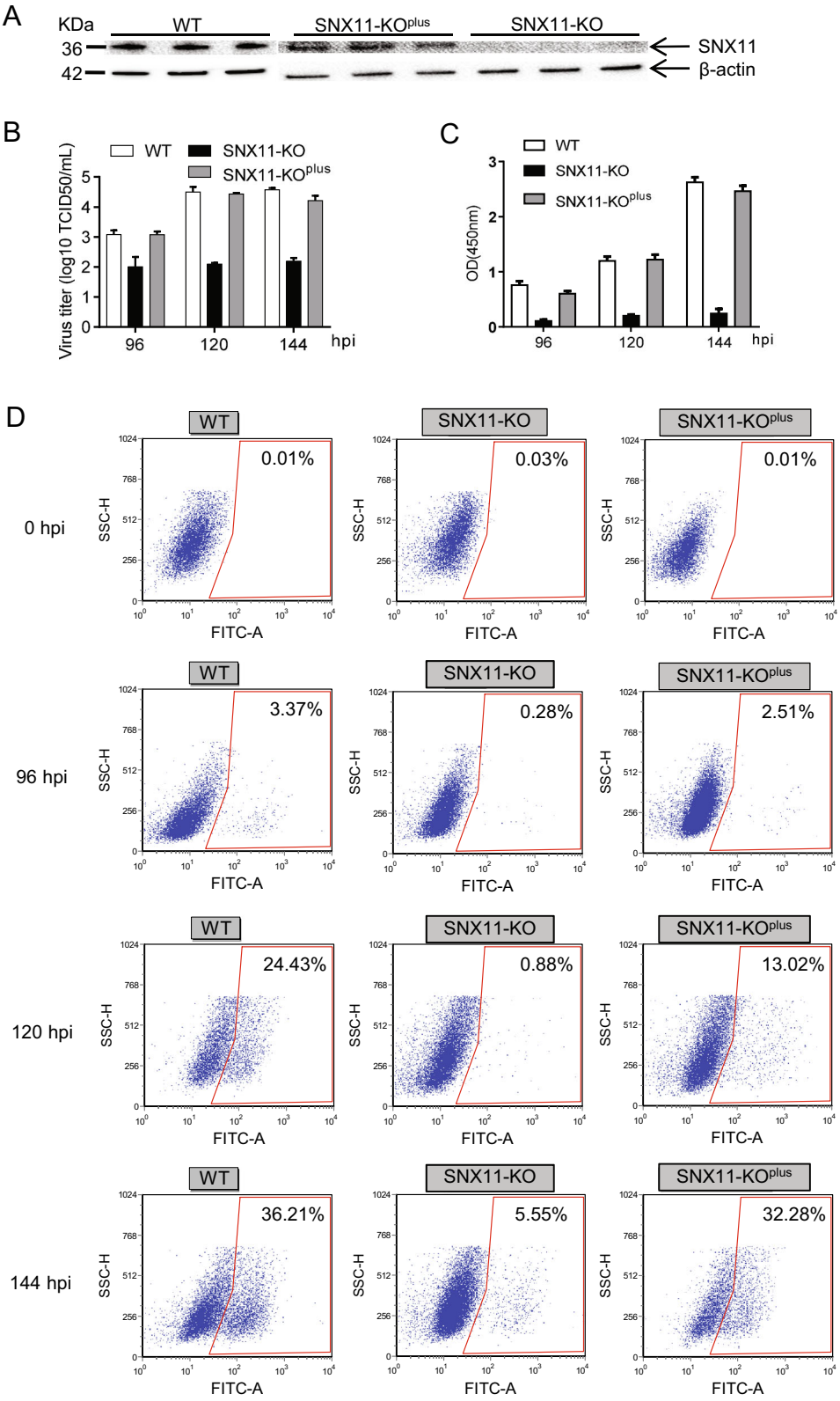

Fig. 2 Confirmation of the reduced and rescued SFTSV infection in the SNX11-KO cell line. **A** Western blotting for SNX11 expression in the wild-type (WT). SNX11-KO, and SNX11-KO^{plus} cells with triplicates. Cell lysates were collected, and equal amounts of protein were loaded onto an SDS-PAGE gel. β-Actin was used as the loading control. **B** Real-time PCR analysis for SFTSV RNA titer in the supernatant of the infected cells at 96, 120, and 144 h post-infection. **C** ELISA for SFTSV NP in the supernatant of the infected cells was performed at 96, 120, and 144 h post-infection in the wild-type (WT), SNX11-KO, and SNX11-KO^{plus} cells. **D** Flow-cytometric analysis of the SFTSV-positive rate in wild-type, SNX11-KO, and SNX11-KO^{plus} cells at 96, 120, and 144 h post-infection. The dots in the gates represent SFTSV-positive cells.

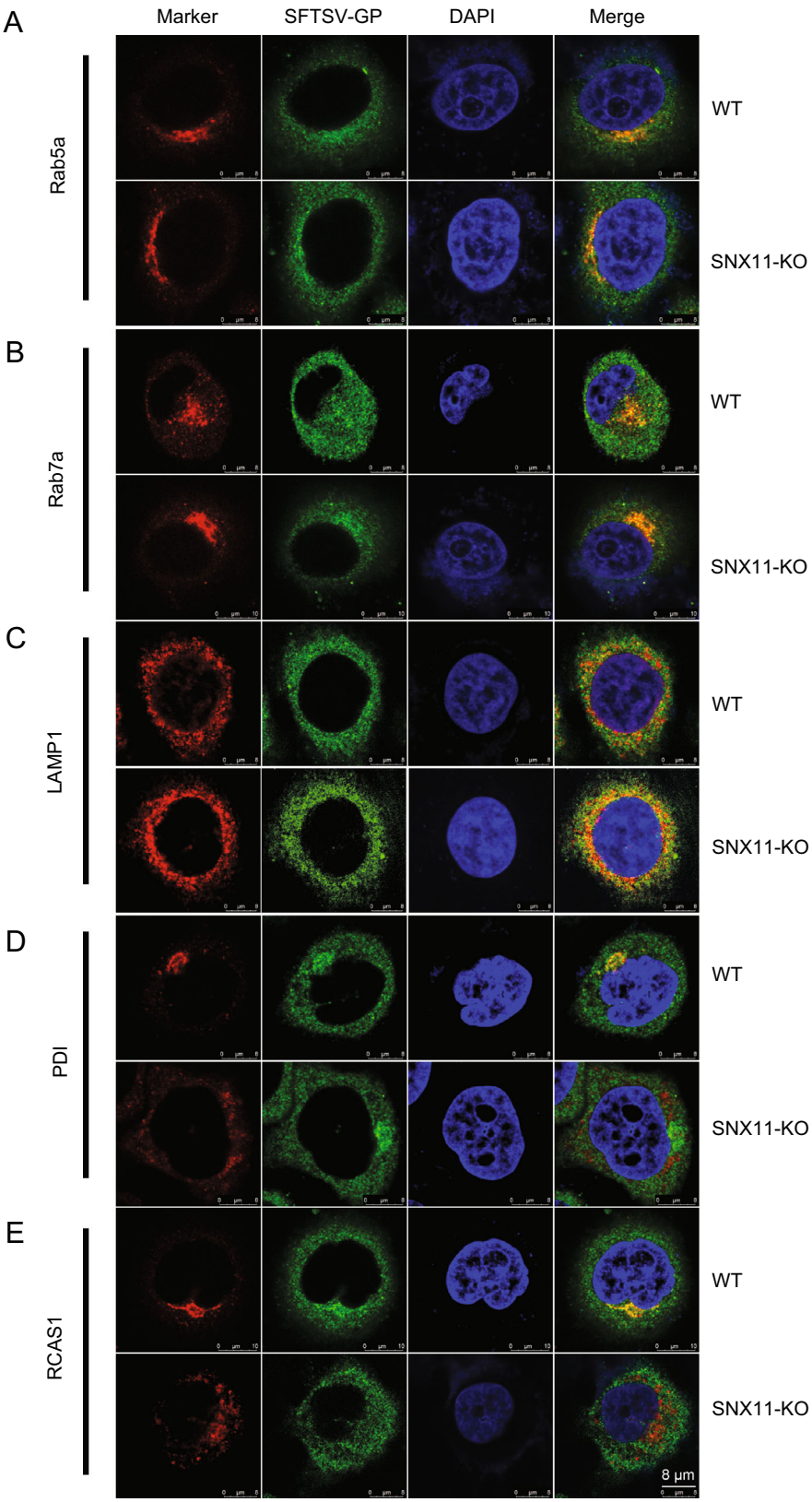

Fig. 3 The colocalization of SFTSV GP with series of organelle markers in the wild-type (WT) and SNX11-KO cells. **A**, **B** Colocalization of SFTSV GP with early endosome and late endosome, respectively. **C** Colocalization of SFTSV GP with endolysosome/lysosome. **D**. **E** Colocalization of SFTSV GP with ER and Golgi apparatus, respectively. Images were acquired with a 63× objective.

SNX11-Knockout Reduced SFTSV Infection by Affecting Membrane Fusion

We were interested in how the knockout of SNX11 blocked the penetration of SFTSV. Thus, we added a fluorescent acidotropic BB cell Probe P02 (Bestbio, China), which was labeled with fluorescein and the fluorescence intensity increased with acidification of the endosomal compartments of the wild-type and SNX11-KO HeLa cells. Then, we analyzed them with dual-fluorescence flow cytometry. The ratio (R value) of fluorescein emissions when the cells were excited by light at wavelengths of 540 nm (F540) and 440 nm (F440) were inversely proportional to the pH value. This experiment used the R value to measure pH. Our results indicated that the F540/F440 ratio of wild-type cells was 5.79, while it was 4.57 in the SNX11-KO cells (Fig. 4A), which suggested that the pH inside the endosomal compartments of the SNX11-KO cells was higher than in those of the wild-type cells. To examine the specific pH values in both wild-type and SNX11-KO cells, a standard curve of the ratio of F540/F440 (Y axis) versus pH values (X axis), was made with a standard pH calibration buffer in a pH range of 2.8–5.8 (Lin *et al.* 2001), and the pH values were calculated from the linear relationship (correlation coefficient 0.9934) between F540/F440 and the pH value. Results showed that the pH of the endosomal compartments in the wild-type cells was 5.33, whereas it was 5.56 in SNX11-KO cells (Fig. 4B), suggesting that the knockout of SNX11 led to a pH increase of 0.23 in the endosomal compartments of the SNX11-KO cells. We used confocal microscopy to explore the interaction between SNX11 and V-ATPase, major proton pumps involved in proton homeostasis of the intracellular compartments. Our results showed that SNX11 colocalized with V-ATPase (Fig. 4C), which provided insight into the mechanism by which SNX11 affected acidification of the endosomal compartments.

To determine whether the knockout of SNX11 affected the formation of early endosome, late endosome, endolysosome, or lysosome, we performed RNA sequencing analysis to compare the mRNA transcription of RAB5a, RAB7a, and LAMP1 from the wild-type and SNX11-KO cells, which showed no significant differences in the levels of RAB5a or RAB7a in the cells (Fig. 5A, left and middle). LAMP1 mRNA was elevated by nearly 50% in the SNX11-KO cells (Fig. 5A, right). Further, we used flow cytometric analysis to compare the protein expression of RAB5a, RAB7a, and LAMP1 in the two kinds of cells, and we found that a significant increase in LAMP1 was also detected in SNX11-KO cells (Fig. 5B, right). A Western blotting analysis supported these findings (Fig. 5C). This increase in LAMP1 expression suggested that the knockout of SNX11 might be caused by changes in the late endosomal compartment, which was closely

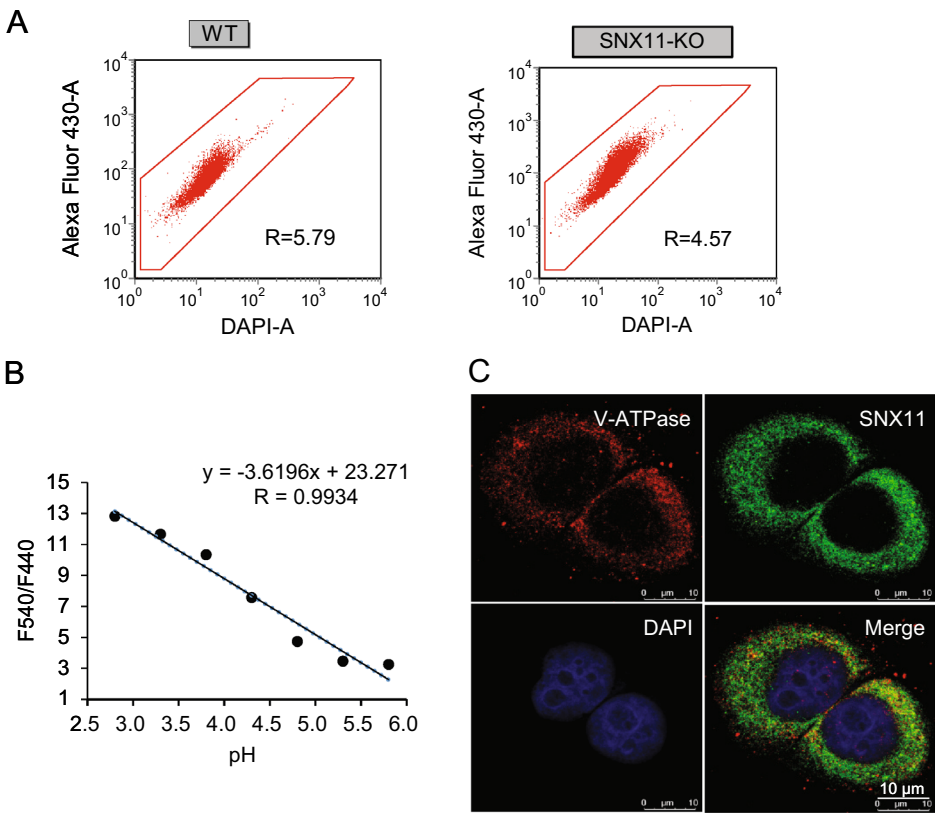

Fig. 4 Increased pH in the endosomal compartments of the SNX11-KO cells. **A** Flow-cytometric analysis of the ratio (R-value) of fluorescein emission when excited by 540 and 440 nm light (F540/F440) in the wild-type (WT) and SNX11-KO cells. **B** The linear relationship between F540/F440 and pH range 2.8–5.8. "R" represents the coefficient of correlation. **C** SNX11 colocalized with V-ATPase.

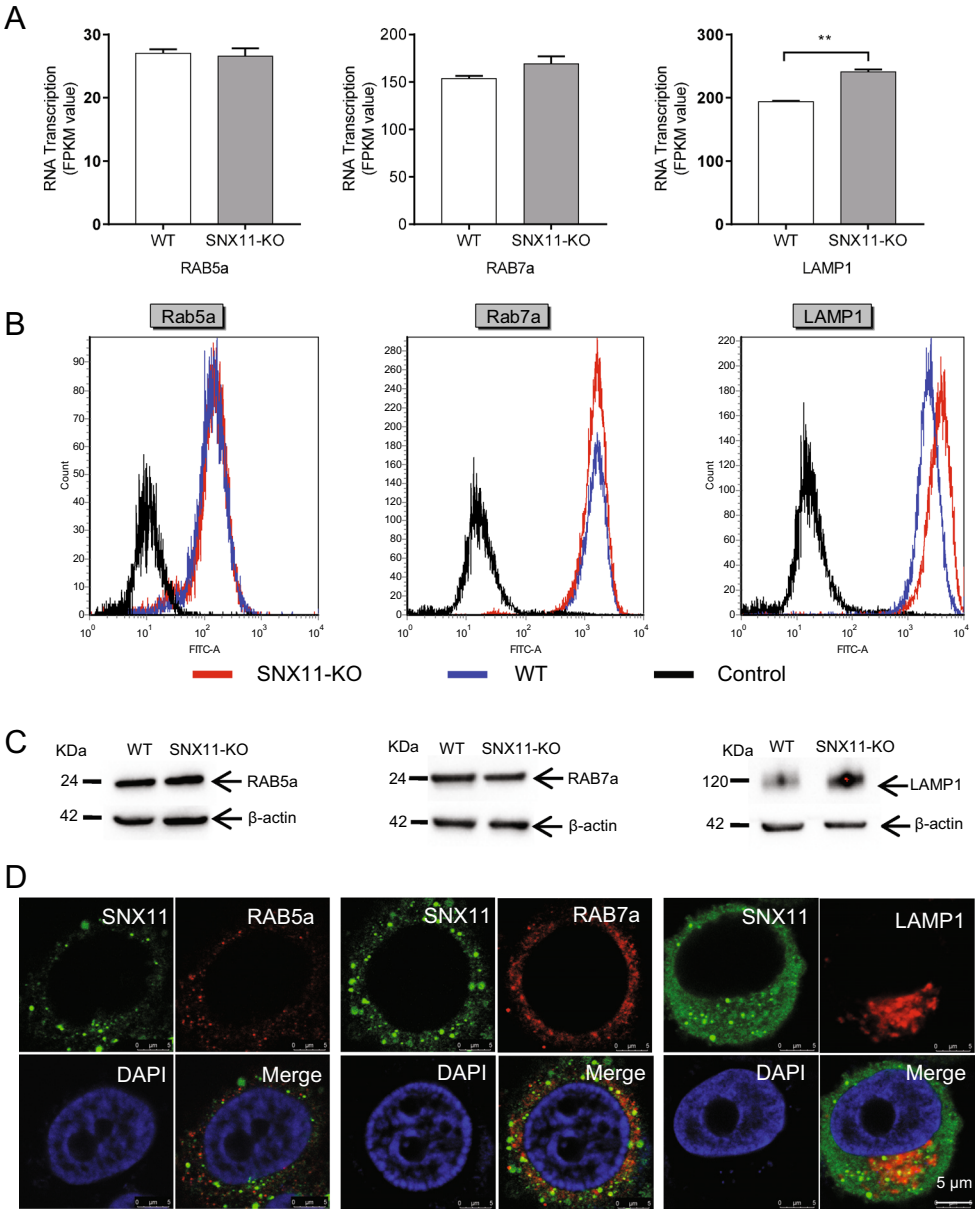

Fig. 5 Increased LAMP1 in SNX11-KO cells. **A** RNA sequencing result for mRNA transcription of RAB5a (left), RAB7a (middle) and LAMP1 (right), in SNX11-KO and wild-type cells (WT), $^{**}P < 0.01$. **B** Flow-cytometric histograms of the expression of RAB5a (left), RAB7a (middle), and LAMP1 (right). Proteins in SNX11-KO (red) and wild-type cells (blue). FITC-A represented the expression level of the specific protein. Secondary antibody control is also shown (black). **C** Western blotting results for the expression of RAB5a (left), RAB7a (middle), and LAMP1 (right) in two kinds of cells, β-actin was added as the loading control. **D** Colocalization of SNX11 with RAB5a, RAB7a, and LAMP1, respectively.

associated with the cytoplasmic penetration of bunyaviruses (Albornoz *et al.* 2016). Therefore, we performed confocal microscopy to investigate the colocalization of SNX11 with RAB5a, RAB7a, and LAMP1, and the results showed that SNX11 was mainly colocalized with RAB7a and LAMP1, while it seldom colocalized with RAB5a (Fig. 5D), which indicated that the late endosomal compartments could be where SNX11 functioned. Further, we used electron microscopy to examine changes in the vesicles by the SNX11-KO cells. The results showed that the endolysosomes had increased within the SNX11-KO cells (Fig. 6).

Discussion

In this study, we used genome-wide CRISPR-based screening to identify the host cellular factors required for SFTSV infection, and a vesicular trafficking protein sorting nexin 11 (SNX11) was identified as essential for the establishment of SFTSV infection, particularly for penetration from the endolysosome to the cytoplasm.

CRISPR-based screening has been widely used to screen host genes in different intracellular signal pathways, particularly for endocytosis, or the ER pathways (Marceau *et al.* 2016; Zhang *et al.* 2016). Screening methods utilized previously were performed via a pooled approach that relied upon gene disruption and stringent selection for

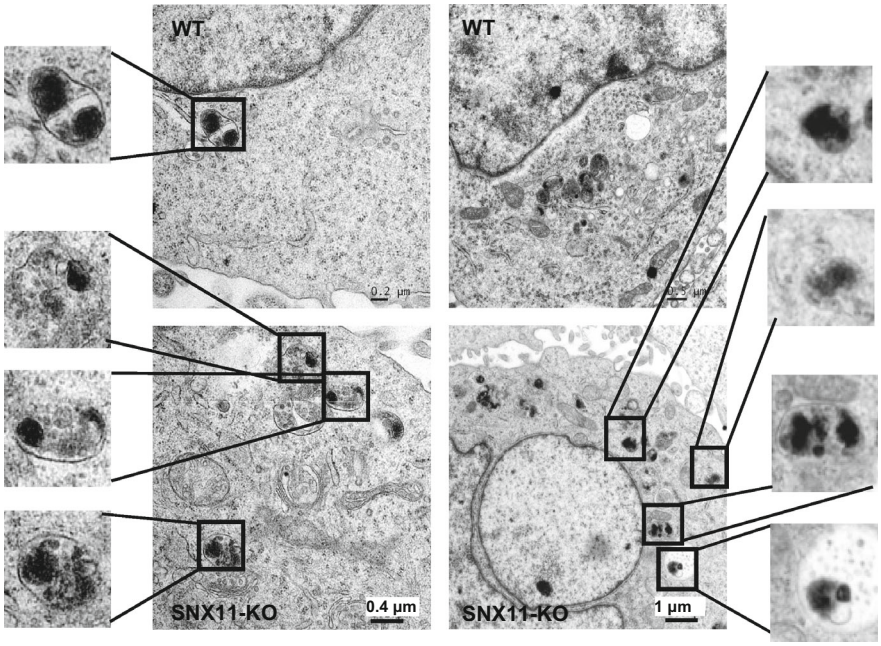

Fig. 6 An electron-microscopic analysis detected significantly increased endolysosomes in SNX11-KO cells. The vesicles highlighted in black boxes are endolysosomes. Images are shown on a map scale of 0.2 μm (left panel) or 0.5 μm (right panel).

enriched cell populations that were resistant to the viral infection in order to obtain a cluster of genes related to a specific pathway. However, this method was not suitable for SFTSV because this infection does not cause cell death; instead, it imparts a mild cytopathic effect (CPE) (Yu *et al.* 2011). In this study, we performed a screen utilizing 96-well plates with limited dilutions of cells, and the advantage of this screening method was that it could isolate a single gene while the disadvantages were that it was difficult to find a cluster of genes that were involved in a single pathway and it was very time-consuming.

In this research, we chose SNX11, a member of the sorting nexins (SNXs) family, for functional study, because this gene contained phox homology (PX) domain and was supposed to be closely related to the endocytic pathway (Seet and Hong 2006). SNXs exert their function through PX-domain-mediated interaction with phosphatidylinositols (PIs), which were abundant in intracellular membranes of the endosomal vesicles such as the early endosomes, late endosomes, and the lysosomes (Seet and Hong 2006). Thus, SNXs are considered to be involved in endosomal membrane trafficking. However, the molecular functions of most of SNXs are still unclear. The first SNX member, SNX1, played a critical role in the down-regulation of EGFR by trafficking it from early endosomes to late endosomes/lysosomes (Kurten *et al.* 1996). There was very limited information available about the function of SNX11 except for a recent report which stated that SNX11 regulated lysosomal degradation of the plasma membrane TRPV3 via targeting from the plasma membrane to the lysosome (Li *et al.* 2016). Thus far, no literature had described the functions of SNX11 in relation to viral infection. Moreover, the intracellular endocytosis processes and the molecular basis of SFTSV infection remained uncharacterized. A recent study (Liu *et al.* 2018) provided a very detailed description of SFTSV entry via endosomal trafficking and penetration. Further, this study found a clathrin-dependent entry of SFTSV and showed that the endocytosed enveloped virions were delivered to Rab5+ early endosomes more often than to Rab7+ late endosomes when membrane fusion was triggered by an acidic environment (Liu *et al.* 2018). However, our results showed that the SFTSV glycoprotein could colocalize with LAMP1, a membrane protein mainly distributed in the endolysosome or lysosome, which suggested that SFTSV might travel deeper into the endolysosomes with more acidic environments than with later endosomes. The endolysosomes are key hybrid organelles formed by the fusion of late endosomes and lysosomes (Huotari and Helenius 2011) and an important compartment for viral trafficking as they provided a more acidic environment for late-penetrating viruses and helped them either penetrate to the cytoplasm or pass to be degraded by the lysosomes (Lozach *et al.* 2011; Albornoz *et al.* 2016). In our study, increased expression of LAMP1 (in spite of RAB5a and RAB7a) indicated that the knockout of SNX11 caused changes in the late endosomal compartments which were closely related to SFTSV penetration. However, the mechanism by which the knockout of SNX11 affected the expression of LAMP1 was not clear. Our results found that SNX11 mainly colocalized with RAB7a and LAMP1, which suggested that the late endosomal compartments might be the place where SNX11 functioned. We then performed electron microscopy which showed that the

endolysosomes had increased in the SNX11-KO cells. Therefore, we speculated that the knockout of SNX11 caused an increase in the pH of the endosomal compartments, blocking release of their cargo (including viruses) into the cytoplasm, and thus, the endolysosomes could not be converted to lysosomes. This would cause excessive accumulation of endolysosomes and could explain the increase in LAMP1. Since there have been no reports of viruses that penetrate from the lysosome (Lozach *et al.* 2011), we speculated that SFTSV might instead enter via the endolysosome, the place where virus penetration occurred. Moreover, our results showed that SFTSV glycoproteins were not detected in the ER or Golgi apparatus in SNX11-KO cells and that the viral RNA load was significantly decreased in the supernatants of SNX11-KO cells, suggesting that penetration of SFTSV virions could be blocked by the endolysosomes.

Further, for most of the bunyaviruses, the endosomal pH was the critical signal for triggering membrane fusion (Albornoz *et al.* 2016). Endosomes, in which the pH changed from $\sim$ 6.5 (early endosomes) down to $\sim$ 5.5–5.0 (later endosome and lysosomes), provided the critical acidic environment for viral penetration. Enveloped viruses penetrated the cytoplasm via membrane fusions between viral and cellular membranes. Our results showed that a knockout of SNX11 led to an increase in the pH value inside the endosomal compartments. While pH only increased minimally in the SNX11-KO cells (pH 5.56) in comparison with wild-type cells (pH 5.33), this sensitive change might have affected functions of the proteases during membrane fusion, indicating that SNX11 may be required for maintaining the acidic environment of later endosomal compartments. Our findings revealed a co-localization between SNX11 and vacuolar H+ ATPase (V-ATPase), which provided additional information regarding the acid-maintaining mechanism. Although endosomal pH is a critical signal for triggering membrane fusion with enveloped viruses, it was sometimes not sufficient (Albornoz *et al.* 2016). Other mechanisms involved with virus penetration included virus glycoproteins cleavage, intracellular interactions with inner receptors, or specific lipids in SFTSV that targeted later endosomal membranes. In the Ebola virus (which has been reported to enter the cytoplasm through endolysosomes), a low endosomal pH was needed to facilitate conformational changes in the primed GP, and an intracellular receptor NPC1 located in the endolysosome membrane was required to trigger membrane fusion followed by virus penetration (Simmons *et al.* 2016). Interestingly, LAMP1 can increase the efficiency of the Lassa virus infection, and the interactions between LAMP1 and the viral mature glycoprotein spike promote Lassa virus membrane fusion and penetration from endolysosomes into the cytosol (Hulseberg *et al.* 2018). Since SFTSV penetration was reported to involve cleavage of the viral envelope glycoproteins Gn and Gc (Hofmann *et al.* 2013), we speculated that SFTSV might utilize the same mechanism as that of the Ebola virus or Lassa virus, but the intracellular receptor of SFTSV has not been elucidated. SNX11 is a protein involved in intracellular trafficking with a specific defined structure in the PX domain. SNX11 binding characteristics such as PIs, which are the most abundant in the intracellular membrane, could act as a carrier or regulating protein affecting the binding process of the cleaved glycoproteins via an unknown intracellular receptor located in the endolysosomes which contributed to viral penetration from the endolysosomes to the cytoplasm.

In conclusion, our findings revealed that SNX11 is an essential host cellular factor for SFTSV infection. Virus penetration was aborted in endolysosomes in SNX11 lacking cells. However, the molecular functions of SNX11 via the intracellular trafficking pathway are poorly characterized, and more solid evidence is required to investigate and explore interactions. Furthermore, regulation of this particular cellular protein during the whole process of SFTSV infection, including entry, endocytic trafficking, penetration, replication, assembly, and maturation, needs to be clarified. We also believe that SNX11 may play an important role in the infection processes of other enveloped viruses, which requires urgent attention in future research.

Acknowledgements This work was supported by the National Key Project for Infectious Disease from the Ministry of Science and Technology (Grant No. 2018ZX10711-001).

Author Contributions TL performed the experiments and wrote the paper; Jiajia Li, YL, and YQ performed the experiments; AL, QZ, CL, WW, YL, and Jiandong Li contributed reagents/materials/analysis tools. Jiajia Li, TL, ML, YL, Jiandong Li, and DL analyzed and discussed the data. ML and SW designed the project and edited the manuscript. All authors read and approved the final manuscript.

Compliance with Ethical Standards

Conflict of interest The authors declare that they have no conflict of interest.

Animal and Human Rights Statement This article does not contain any studies with human or animal subjects performed by any of the authors.

References

Albornoz A, Hoffmann AB, Lozach PY, Tischler ND (2016) Early bunyavirus-host cell interactions. Viruses 8:143

De Boer SM, Kortekaas J, Spel L, Rottier PJ, Moormann RJ, Bosch BJ (2012) Acid-activated structural reorganization of the Rift Valley fever virus Gc fusion protein. J Virol 86:13642–13652

Han J, Perez JT, Chen C, Li Y, Benitez A, Kandasamy M, Lee Y, Andrade J, tenOever B, Manicassamy B (2018) Genome-wide CRISPR/Cas9 screen identifies host factors essential for influenza virus replication. Cell Rep 23:596–607

Heaton BE, Kennedy EM, Dumm RE, Harding AT, Sacco MT, Sachs D, Heaton NS (2017) A CRISPR activation screen identifies a pan-avian influenza virus inhibitory host factor. Cell Rep 20:1503–1512

Hofmann H, Li X, Zhang X, Liu W, Kuhl A, Kaup F, Soldan SS, Gonzalez-Scarano F, Weber F, He Y, Pohlmann S (2013) Severe fever with thrombocytopenia virus glycoproteins are targeted by neutralizing antibodies and can use DC-SIGN as a receptor for pH-dependent entry into human and animal cell lines. J Virol 87:4384–4394

Hulseberg CE, Fénéant L, Szymańska KM, White JM (2018) Lamp1 increases the efficiency of lassa virus infection by promoting fusion in less acidic endosomal compartments. Mbio 9:e01818-01817

Huotari J, Helenius A (2011) Endosome maturation. EMBO J 30:3481–3500

Jin M, Park J, Lee S, Park B, Shin J, Song KJ, Ahn TI, Hwang SY, Ahn BY, Ahn K (2002) Hantaan virus enters cells by clathrin-dependent receptor-mediated endocytosis. Virology 294:60–69

Kim K-H, Yi J, Kim G, Choi SJ, Jun KI, Kim N-H, Choe PG, Kim N-J, Lee J-K, Oh M-d (2013) Severe fever with thrombocytopenia syndrome, South Korea, 2012. Emerg Infect Dis 19:1892–1894

Kurten RC, Cadena DL, Gill GN (1996) Enhanced degradation of EGF receptors by a sorting nexin, SNX1. Science 272:1008–1010

Li C, Ma W, Yin S, Liang X, Shu X, Pei D, Egan TM, Huang J, Pan A, Li Z (2016) Sorting nexin 11 regulates lysosomal degradation of plasma membrane TRPV3. Traffic 17:500–514

Lin HJ, Herman P, Kang JS, Lakowicz JR (2001) Fluorescence lifetime characterization of novel low-pH probes. Anal Biochem 294:118–125

Liu J, Xu M, Tang B, Hu L, Deng F, Wang H, Pang DW, Hu Z, Wang M, Zhou Y (2018) Single-particle tracking reveals the sequential entry process of the bunyavirus severe fever with thrombocytopenia syndrome virus. Small. https://doi.org/10.1002/smll.201803788:e1803788

Lozach PY, Mancini R, Bitto D, Meier R, Oestereich L, Overby AK, Pettersson RF, Helenius A (2010) Entry of bunyaviruses into mammalian cells. Cell Host Microbe 7:488–499

Lozach PY, Huotari J, Helenius A (2011) Late-penetrating viruses. Curr Opin Virol 1:35–43

Ma H, Dang Y, Wu Y, Jia G, Anaya E, Zhang J, Abraham S, Choi JG, Shi G, Qi L, Manjunath N, Wu H (2015) A CRISPR-based screen identifies genes essential for West-Nile-virus-induced cell death. Cell Rep 12:673–683

Marceau CD, Puschnik AS, Majzoub K, Ooi YS, Brewer SM, Fuchs G, Swaminathan K, Mata MA, Elias JE, Sarnow P, Carette JE (2016) Genetic dissection of *Flaviviridae* host factors through genome-scale CRISPR screens. Nature 535:159–163

Mayor S, Parton RG, Donaldson JG (2014) Clathrin-independent pathways of endocytosis. Cold Spring Harb Perspect Biol 6:a016758

McMullan LK, Folk SM, Kelly AJ, Macneil A, Goldsmith CS, Metcalfe MG, Batten BC, Albariño CG, Zaki SR, Rollin PE (2012) A new phlebovirus associated with severe febrile illness in Missouri. N Engl J Med 367:834–841

Park RJ, Wang T, Koundakjian D, Hultquist JF, Lamothe-Molina P, Monel B, Schumann K, Yu H, Krupzcak KM, Garcia-Beltran W, Piechocka-Trocha A, Krogan NJ, Marson A, Sabatini DM, Lander ES, Hacohen N, Walker BD (2017) A genome-wide CRISPR screen identifies a restricted set of HIV host dependency factors. Nat Genet 49:193–203

Plegge T, Hofmann-Winkler H, Spiegel M, Pohlmann S (2016) Evidence that processing of the severe fever with thrombocytopenia syndrome virus Gn/Gc polyprotein is critical for viral infectivity and requires an internal Gc signal peptide. PLoS ONE 11:e0166013

Seet LF, Hong W (2006) The Phox (PX) domain proteins and membrane traffic. Biochim Biophys Acta 1761:878–896

Simmons JA, D'Souza RS, Ruas M, Galione A, Casanova JE, White JM, Dermody TS (2016) Ebolavirus glycoprotein directs fusion through $NPC1^{+}$ endolysosomes. J Virol 90:605–610

Sun Y, Qi Y, Liu C, Gao W, Chen P, Fu L, Peng B, Wang H, Jing Z, Zhong G, Li W (2014) Nonmuscle myosin heavy chain IIA is a critical factor contributing to the efficiency of early infection of severe fever with thrombocytopenia syndrome virus. J Virol 88:237–248

Takahashi T, Maeda K, Suzuki T, Ishido A, Shigeoka T, Tominaga T, Kamei T, Honda M, Ninomiya D, Sakai T (2014) The first identification and retrospective study of severe fever with thrombocytopenia syndrome in Japan. J Infect Dis 209:816–827

Tani H, Shimojima M, Fukushi S, Yoshikawa T, Fukuma A, Taniguchi S, Morikawa S, Saijo M (2016) Characterization of glycoprotein-mediated entry of severe fever with thrombocytopenia syndrome virus. J Virol 90:5292–5301

Yu XJ, Liang MF, Zhang SY, Liu Y, Li JD, Sun YL, Zhang L, Zhang QF, Popov VL, Li C, Qu J, Li Q, Zhang YP, Hai R, Wu W, Wang Q, Zhan FX, Wang XJ, Kan B, Wang SW, Wan KL, Jing HQ, Lu JX, Yin WW, Zhou H, Guan XH, Liu JF, Bi ZQ, Liu GH, Ren J, Wang H, Zhao Z, Song JD, He JR, Wan T, Zhang JS, Fu XP, Sun LN, Dong XP, Feng ZJ, Yang WZ, Hong T, Zhang Y, Walker DH, Wang Y, Li DX (2011) Fever with thrombocytopenia associated with a novel bunyavirus in China. N Engl J Med 364:1523–1532

Zhan J, Wang Q, Cheng J, Hu B, Li J, Zhan F, Song Y, Guo D (2017) Current status of severe fever with thrombocytopenia syndrome in China. Virol Sin 32:51–62

Zhang R, Miner JJ, Gorman MJ, Rausch K, Ramage H, White JP, Zuiani A, Zhang P, Fernandez E, Zhang Q, Dowd KA, Pierson TC, Cherry S, Diamond MS (2016) A CRISPR screen defines a signal peptide processing pathway required by flaviviruses. Nature 535:164–168